THE ASTROPHYSICAL JOURNAL, 200:660–674, 1975 September 15


# STELLAR MODEL CHROMOSPHERES. III. ARCTURUS (K2 III)

T. R. AYRES AND J. L. LINSKY*
Joint Institute for Laboratory Astrophysics, University of Colorado and National Bureau of Standards, Boulder
*Received 1974 December 23*

## ABSTRACT

We construct models for the upper photosphere and chromosphere of Arcturus based on the H, K, and IR triplet lines of Ca II and the *h* and *k* lines of Mg II. The chromosphere model is derived from complete redistribution solutions for a five-level Ca II ion and a two-level Mg II ion. A photospheric model is derived from the Ca II wings using first the "traditional" complete redistribution limit and then the more realistic partial redistribution approximation. In particular, the temperature and mass column densities for the temperature minimum region and the chromosphere-transition region boundary are computed and the pressure $P_0$ in the transition region and corona estimated. We find $T_{\rm min}/T_{\rm eff} \approx 0.77$ for Arcturus, Procyon, and the Sun and a trend of increasing mass at the temperature minimum with decreasing gravity. We find $P_0$ to be about 1 percent of the solar value, and on this basis estimate the surface brightness of the Arcturus transition region and coronal spectrum to be much less than for the Sun. Finally, the partial redistribution calculation for the Ca II K line indicates that the emission width is at least partially determined by damping rather than Doppler broadening, suggesting a reexamination of previous explanations for the Wilson-Bappu effect.

*Subject headings:* atmospheres, stellar — Ca II emission — chromospheres, stellar — radiative transfer — stars, individual

## I. INTRODUCTION

In the previous paper of this series (Ayres, Linsky, and Shine 1974, hereafter Paper II), we discussed a grid of possible chromospheric models for the F5 subgiant Procyon, based on calibrated profiles of the Ca II K and Mg II *k* resonance lines and the Ca II subordinate line λ8542. Our major conclusion was that Procyon's average chromosphere (temperature and microvelocity versus mass column density) is qualitatively and quantitatively similar to the Sun's, although Procyon's temperature minimum was found to occur at a higher temperature and at a larger mass column density than the solar temperature minimum.

In this paper we apply the techniques presented in Paper II to the Ca II H and K lines (3969, 3934 Å); the analogous Mg II *h* and *k* lines (2803, 2796 Å); and the Ca II subordinate infrared triplet (8498, 8542, 8662 Å) of the K2 giant Arcturus. We then reconsider the photospheric model taking partial redistribution effects (e.g., Milkey, Ayres, and Shine 1975*a*) into account. Since Arcturus is a metal-deficient, high-velocity star (Roman 1952, 1955; Conti *et al.* 1967; Griffin and Griffin 1967; Gustafsson, Kjaergaard, and Anderson 1974; Simon 1970; Simon, Morrison, and Cruikshank 1972; Greene 1969), we might expect its mild Population II character to produce a qualitatively different stellar chromosphere from that of the Sun or Procyon. Arcturus does show a much larger emission contrast in Ca II H and K than either the Sun or Procyon, but similar to other K giants. More unusual is the appearance of a weak emission feature in the near wing of Ca II H attributed to the Balmer line Hε (Wilson 1938, 1957). In both the Sun and Procyon this feature is seen in absorption. In addition, the Arcturus $K_2$ emission strength is known to vary appreciably (10–20%) on time scales of hours and days (Griffin 1963; Liller 1968), although periodicities analogous to the familiar solar activity cycle have not yet been seen. Ca II $K_{2r}$–$K_{2v}$ asymmetries have been observed on similar time scales (Liller 1968), and the moderate-resolution (~0.4 Å) *Copernicus* profiles of the far-ultraviolet Mg II *h* and *k* and Lα lines (Moos *et al.* 1974) show marked red-peak enhancements. These asymmetries, especially in the more opaque Lα and *h* and *k* lines, suggest the presence of a strong stellar wind analogous to the solar wind, or large-scale mass motions in Arcturus's chromosphere. Similar asymmetries are seen in the Mg II and Lα lines of the K5 giant Aldebaran (Linsky *et al.* 1975). We note that if strong vertical motions are present in the low chromosphere of Arcturus, models based on hydrostatic equilibrium—such as the ones we construct below—may be an inadequate description of an essentially hydrodynamic situation.

Our major concern in this paper is to derive an "average" model of the upper photosphere and low chromosphere of Arcturus within the constraints imposed by the lack of spatial and temporal information in the observed line profiles, uncertainties in the absolute calibrations, and simplifications in the radiative transfer solutions. Since the limitations of our models may tend to cancel in a differential comparison with similar models for the Sun, Procyon, and other

* Staff Member, Laboratory Astrophysics Division, National Bureau of Standards.

stars, we apply basically the same techniques described in Paper II, although we have introduced several important modifications based on insights gained during the course of our investigation of Arcturus and from the recent work on redistribution functions by Milkey and Mihalas (1973*a*, 1974) and others.

The paper is divided into sections as follows: Section II is devoted to the observation and calibration of chromospheric lines in Arcturus's spectrum. In § III we construct upper-photosphere/low-chromosphere models assuming complete redistribution to fit the observations of § II. In § IV we discuss the effects of partial frequency redistribution in the inner wings of the K line on the inferred photospheric temperature model. Finally in § V we comment on the significance of our findings for the understanding of stellar chromosphere phenomena.

## II. OBSERVATIONS

### *a*) Ca II H *and* K: *Griffin's Atlas*

Only a small group of bright stars have been observed with spectral resolution adequate to fully resolve the Ca II H and K emission cores—at least $\lambda/\Delta\lambda \sim 100{,}000$ for solar-type stars, but somewhat less for giants and supergiants which usually show broader emission than main-sequence stars (i.e., the Wilson-Bappu effect [Wilson and Bappu 1957]). Arcturus is one of these stars by virtue of Griffin's extensive *Photometric Atlas* (Griffin 1968). In these data the spectral resolution at H and K and the infrared triplet exceeds 100,000, and stray light—due to grating ghosts and diffuse scattered light—is stated to be low and in this work is assumed to be zero. The latter consideration is particularly important for H and K because a large stray light level can confuse the interpretation of the line core and inner wing intensities which are generally on the order of only a few percent of the neighboring "continuum" intensities.

### *b*) *Calibration of* H *and* K

Willstrop (1965, 1972) has measured the flux at the Earth in narrow bands (50 Å) of Arcturus's spectrum. We adopt an angular diameter of 0".023 ± 5 percent (Simon *et al.* 1972) and $V = 0.06$ (Hoffleit 1964) to convert Willstrop's measurements to absolute units per cm$^2$ of the stellar surface. Such a calibration is essential for comparing the observed profiles with fluxes predicted by model chromosphere calculations. We note that this absolute calibration is consistent to within about 4 percent of the scales established by Oke (1964) and Hayes (1967) for Vega near 4000 Å (Latham 1970).

In order to apply this calibration to Griffin's profiles of Ca II H and K we chose three of Willstrop's bands centered at 3925, 3950, and 3975 Å and planimetered the corresponding 50 Å bands in Griffin's Atlas to determine the conversion factor going from relative to absolute flux. We found a reasonably good

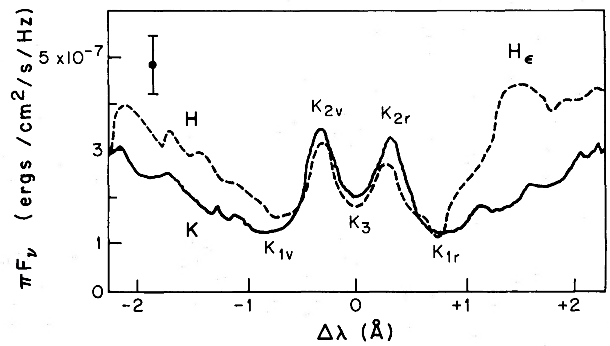


FIG. 1.—Calibrated flux profiles of the Arcturus Ca II H and K lines. The $K_1$, $K_2$, and $K_3$ features and the hydrogen H$\epsilon$ line are indicated.

agreement between the calibration factors for each band. We then applied the calibration to digitized sections of the H and K cores and inner wings, taking an average of the adjacent calibration factors for each line. The resulting calibrated profiles of H and K are shown in Figure 1. In this figure, H$\epsilon$ can be seen prominently in emission at +1.6 Å from H line-center. The error bars refer to the 20–30 percent uncertainty in the absolute calibration. These uncertainties arise from several sources: (1) the stellar angular diameter which enters quadratically in the geometrical dilution factor (±10 percent); (2) Willstrop's photometry (±10 percent); and (3) in the averaging of the calibration factors (±10 percent for K, ±1 percent for H).

The flux in each line core integrated over a ±0.75 Å bandpass about line center ($K_{1v}$–$K_{1r}$) is $\pi F_K = 6.8 \times 10^4 \pm 30$ percent ergs cm$^{-2}$ s$^{-1}$ and $\pi F_H = 6.7 \times 10^4 \pm 20$ percent ergs cm$^{-2}$ s$^{-1}$. The corresponding values for K lines of the Sun and Procyon (±0.5 Å bandpass) are $\pi F_K = 7.5 \times 10^5 \pm 10$ percent and $\pi F_K = 1.9 \times 10^6 \pm 20$ percent, respectively. Note that although both the "emission contrast" $\{\pi F_{K_2}/\pi F_{K_1}\}$ and $K_{1v} - K_{1r}$ bandpass are greater for the Arcturus K line, the integrated flux is much less than for either the Sun or Procyon.

### *c*) *The* Ca II *Infrared Triplet*

Although the cores of the Ca II subordinate lines are not as sensitive to the details of the chromospheric temperature inversion as H and K, the infrared triplet lines provide an important consistency check for the five-level + continuum radiative-transfer/statistical-equilibrium calculations, as well as sensitive microvelocity indicators. Furthermore, like H and K, the profiles of the damping wings of the infrared lines are largely determined by the temperature structure of the upper photosphere. Because a reliable infrared calibration is not available for Griffin's profiles of 8498, 8542, and 8662 Å, we calibrate the chromospheric cores of the subordinate lines by fitting the observed damping wings with theoretical fluxes (line wing + background continuum) based on an upper photosphere model derived from the H and K inner wings (see § III*a*, below).

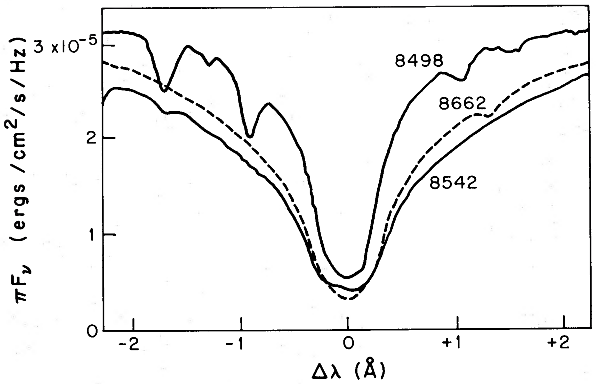


FIG. 2.—Calibrated flux profiles of the Arcturus Ca II subordinate infrared triplet lines.

The calibrated profiles of the infrared triplet lines are shown in Figure 2.

### *d*) Mg II *h and k*

As has been noted in Paper II and elsewhere (e.g., Kondo *et al.* 1972), the Mg II *h* and *k* resonance lines are very useful probes of chromospheric conditions above the layers of the low chromosphere where the less opaque Ca II H and K lines are formed. Unfortunately, the usefulness of *h* and *k* for inferring chromospheric structure is diminished significantly by the difficulty of calibrating the line profiles in absolute units, although we could base a rough calibration on a technique analogous to that used for the Ca II subordinate lines in the previous section if observations of the *h* and *k* line wings were available.

The Mg II profiles we consider here are from *Copernicus* observations of Arcturus by Moos *et al.* (1974). Unfortunately, the inner wings of *h* and *k* are buried in the high background level of the photometry. Because the *h* and *k* line wings are not available for a differential calibration relative to the high-quality Ca II K line data, we must rely instead on the Moos *et al.* (1974) calibration based on Doherty's (1972) low-resolution OAO-2 observations of Arcturus's ultraviolet spectrum. We caution that this calibration may be in error by a large factor. The calibrated *Copernicus* profiles of *h* and *k* are illustrated in Figure 3. Note the pronounced asymmetries of both *h* and *k*. The integrated fluxes ($\pm 1.0$ Å) are: $\pi F_k = 1.1 \times 10^5$ ergs cm$^{-2}$ s$^{-1}$ and $\pi F_k = 0.8 \times 10^5$ ergs cm$^{-2}$ s$^{-1}$. The accuracy of these fluxes is probably on the order of $\pm 50$ percent. As with H and K, the more opaque and hence more nearly thermalized Arcturus *k* line is brighter than the *h* line.

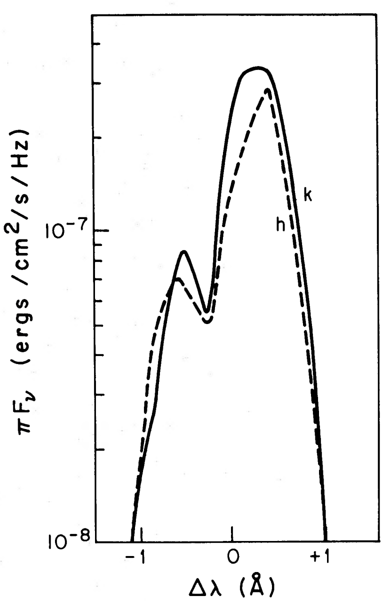


FIG. 3.—Calibrated flux profiles of the Arcturus Mg II *h* (λ2803) and *k* (λ2796) lines.

The corresponding *k* fluxes ($\pm 0.75$ Å) for the Sun (Brinkmann, Green, and Barth 1966) and Procyon (Paper II) are: $\pi F_k^{\odot} = 0.82 \times 10^6$ ergs cm$^{-2}$ s$^{-1}$ and $\pi F_k^{\alpha \mathrm{CMi}} \gtrsim 0.82 \times 10^6$ ergs cm$^{-2}$ s$^{-1}$. We regard the value of $\pi F_k^{\alpha \mathrm{CMi}}$ given above as a lower limit because it is based on a method of scaling the Ca II K line absolute calibration to the Mg II *k* line assuming complete redistribution (see Paper II). A modified version of this method based on the more physical partial-coherent scattering approximation (Ayres 1975) suggests that the complete redistribution calibration of the Procyon *h* and *k* lines given in Paper II may be too low by a factor of approximately 50 percent.

## III. MODEL ATMOSPHERES FOR ARCTURUS ASSUMING COMPLETE REDISTRIBUTION

### *a*) *The Upper Photosphere*

In Paper II we outlined a method for constructing accurate semiempirical $T_e(m)$ ($m$ is the mass column density in grams cm$^{-2}$) models of the upper photospheres of late-type stars using calibrated profiles of the inner wings of Ca II K. This method was originally devised to study the temperature structure of individual solar photospheric faculae without recourse to statistical limb-darkening data (Shine and Linsky 1974*a*).

Accurate empirical models of late-type stellar photospheres are useful for several reasons:

1. There is wide disagreement concerning the role of line blanketing, especially that due to molecular bands in cool stars, in controlling the radiative equilibrium temperature distribution in the upper photosphere and the radiative equilibrium boundary temperature (Carbon and Ridgway 1973; Johnson 1973). Because the layers of a typical late-type stellar photosphere that are most susceptible to line-blanketing-induced temperature perturbations occur at small continuum optical depths, it is often difficult to distinguish two models of similar effective temperature but widely dissimilar upper photosphere structure on the basis of predicted continuum intensities alone. However, two such models could more easily be

distinguished by their effect on the inner wings of the K line, which are formed in the upper photosphere.

2. A knowledge of the temperature minimum, $T_{\rm min}$, and the location of $T_{\rm min}$ in "mass," $m(T_{\rm min})$, are essential for the understanding of the onset of nonradiative heating in the low chromospheres of late-type stars. Apart from the Cayrel mechanism (Cayrel 1963), which allows for a small outward temperature rise via radiative heating, the existence of "chromospheric" and "coronal" temperatures in the Sun and other late-type stars, as suggested by the presence of the He I λ10830 and λ5876 lines (Vaughan and Zirin 1968; Pasachoff and Lepler 1972) and the O V λ1218 line in β Gem (Gerola *et al.* 1974), implies that some degree of nonradiative energy dissipation must be occurring throughout the stellar upper photosphere, temperature minimum, chromosphere, and corona to balance the excess radiative losses in those layers (see Ayres 1975; Ayres and Linsky 1975*b* [Paper V]). Furthermore, the specification of $[T_{\rm min}, m(T_{\rm min})]$ fixes a rough lower boundary condition for the stellar chromospheric temperature rise. This latter point is important because otherwise one is forced to specify the model chromosphere in an entirely ad hoc way—for example, a "scaled" solar model. We note that a previous attempt to construct a chromospheric model for Arcturus based on an analysis of the Na I D lines (Simon 1970) was unsuccessful in producing good profile fits to the core and wings of Ca II K largely because the upper photosphere temperature distribution used was based on theoretical radiative equilibrium (RE) models having boundary temperatures several hundred degrees in excess of Arcturus's probable $T_{\rm min}$.

3. Since the inner wings of the H and K lines broaden with luminosity in essentially the same way as the emission cores (Lutz, Furenlid, and Lutz 1973), it is tempting to suggest that the well-known Wilson-Bappu effect (Wilson and Bappu 1957; Wilson 1966) may be an artifact of the behavior of upper-photosphere structure with gravity rather than a variation of chromospheric microvelocity with luminosity as has traditionally been proposed (e.g., Kraft 1959; Wilson 1966; Fosbury 1973; Reimers 1973; Scharmer 1974). Evidence in favor of a primarily photospheric origin for the Wilson-Bappu effect has been given recently (Ayres *et al.* 1973; Ayres, Linsky, and Shine 1975), and an investigation of this problem based on realistic stellar models such as the one we derive here for Arcturus, and an improved treatment of the redistribution problem (see, e.g., Milkey and Mihalas 1974) is currently under way (cf. Paper V in this series).

### i) *Temperature Models from the K-Line Wings*

A complete discussion of our semiempirical approach based on the brightness temperature profile $T_B(\Delta\lambda)$ of the K line wings can be found in Paper II and elsewhere (e.g., Shine 1973; Shine and Linsky 1974*a*). We outline the basic approach here to explicitly demonstrate the dependence of the derived $T_e(m)$ model on fundamental atomic constants and stellar parameters.

Briefly, we assume that each brightness temperature in the damping wings of the K line $T_B(\Delta\lambda)$, where

$$\pi B_\nu[T_B(\Delta\lambda)] = \pi F_{\Delta\lambda} \tag{1}$$

corresponds to a unique mass point and $T_e(m)$ in the stellar photosphere through the mapping of the thermalized wing source function $[S_\nu^{\rm wing} = B_\nu(T_e)]$ via the Eddington-Barbier relation for the flux, i.e.,

$$T_B(\Delta\lambda) \sim T_e(t_{\Delta\lambda} \sim \tfrac{2}{3})\,. \tag{2}$$

Here $t_{\Delta\lambda}$ is the monochromatic optical depth (wing + continuum) $\Delta\lambda$(Å) from line center. The wing source function is assumed to be in LTE since the line-center optical depths in the photosphere far exceed the complete redistribution thermalization length.

Using the opacity relation for the K line wing including both radiative damping and van der Waals broadening, and assuming that all of the calcium is in the ground state of $Ca^+$, we find the following relation for the mass column density at a given $T_e = T_B(\Delta\lambda)$ (e.g., Paper II):

$$m(\Delta\lambda) \sim \frac{(1+A_{\rm He})\times 5000kT_5^{\,0.7}}{g}\,\frac{\Gamma_{\rm rad}}{\Gamma_{\rm vw}} \times\left\{\left[1+2\frac{\Gamma_{\rm vw}}{\Gamma_{\rm rad}^{\,2}}\,\frac{(\frac{2}{3}-\tau_c)\Delta\lambda^2 g T_5^{\,-0.7}}{\bar\kappa(1+A_{\rm He})5000k}\right]^{1/2}-1\right\}\cdot \tag{3}$$

Here $\Gamma_{\rm vw}$ and $\Gamma_{\rm rad}$ are the damping constants, $\tau_c$ is a correction for continuous opacity, $T_5 \equiv T_B(\Delta\lambda)/5000$, $k$ is Boltzmann's constant, $A_{\rm He}$ is the stellar helium abundance (H = 1), $g$ is the stellar gravity, and

$$\bar\kappa = 5.0 \times 10^{-3} \times A_{\rm Ca}\,, \tag{4}$$

where $A_{\rm Ca}$ is the stellar calcium abundance. A similar expression is valid for the H line except with a $\bar\kappa$ one-half the value given in equation (4) above. When the second term within the square root is small compared with unity, a useful approximation to equation (3) is

$$m(\Delta\lambda) \sim \tfrac{2}{3}\Delta\lambda^2/(\bar\kappa\Gamma_{\rm rad})\,. \tag{5}$$

Equation (5) illustrates an advantage of this approach for low-gravity stars such as Arcturus and other late-type giants: we can derive an upper photosphere model independent of the often poorly known stellar surface gravity. Furthermore, the derived model is insensitive to the van der Waals damping constant $\Gamma_{\rm vw}$, which is less well determined than $\Gamma_{\rm rad}$ (Shine and Linsky 1974*a*). Physically, the weak dependence of $m(\Delta\lambda)$ on gravity and $\Gamma_{\rm vw}$ arises from the relatively minor role played by pressure broadening in a low-density (i.e., low-gravity) stellar photosphere.

However, because the K-wing optical depths depend on the stellar calcium abundance, the accuracy $(\Delta m)$ of the inferred *mass scale* is limited by the accuracy of $[{\rm Fe/H}] \equiv \log\,[A_{\rm Fe}{}^*/A_{\rm Fe}{}^{\odot}]$ measurements for the given star, assuming that [Ca/Fe] is solar.

TABLE 1

MEAN BRIGHTNESS TEMPERATURE AND COMPUTED MASS COLUMN DENSITIES (complete redistribution)

| $\Delta\lambda$ (Å) | $T_B^{\mathrm{K}}$ (K) | $T_B^{\mathrm{H}}$ (K) | $m_{\mathrm{calc}}^{\mathrm{K}}$* (g cm$^{-2}$) | $m_{\mathrm{calc}}^{\mathrm{H}}$ (g cm$^{-2}$) |
|---|---|---|---|---|
| 0.8 | 3052 | 3142 | 8.82(−1) | 1.76 |
| 0.9 | 3060 | 3169 | 1.12 | 2.22 |
| 1.0 | 3076 | 3179 | 1.38 | 2.73 |
| 1.4 | 3124 | 3269 | 2.68 | 5.29 |
| 1.8 | ... | 3335 | ... | 8.63 |
| 2.2 | 3294 | 3394 | 6.50 | 1.27(1) |
| 2.6 | 3320 | 3444 | 8.98 | 1.73(1) |
| 3.2 | 3367 | 3514 | 1.34(1) | 2.54(1) |
| 3.8 | 3438 | ... | 1.84(1) | ... |
| 4.4 | 3490 | 3645 | 2.42(1) | 4.48(1) |
| 4.8 | 3521 | ... | 2.83(1) | ... |
| 5.6 | 3580 | 3741 | 3.73(1) | 6.74(1) |
| 6.2 | 3650 | ... | 4.45(1) | ... |
| 6.6 | ... | 3829 | ... | 8.79(1) |
| 7.1 | 3698 | ... | 5.61(1) | ... |

* $\log g = 1.7$, $A_{\mathrm{Ca}} = 6.42(-7)$, $\Gamma_{\mathrm{vw}} = 1.6(-8)$.

Likewise the accuracy of the inferred *temperatures* ($\Delta T$) is limited by the accuracy of the absolute calibration.

In the following section we propose an upper photosphere model based on the calibrated K wing profiles of § II and the range of physical parameters ($g$, [Fe/H], $T_{\mathrm{eff}}$) inferred from observations of Arcturus.

ii) *The Adopted Upper Photosphere Model*

Table 1 lists the (brightness temperature, $\Delta\lambda$)-relation based on a red-blue average of the H and K wing fluxes of § II. Also given in Table 1 are the inferred column densities for $g = 50$, $[\mathrm{Fe/H}] = -0.50$, and $\Gamma_{\mathrm{vw}} = 1.6 \times 10^{-8}$. We have restricted the $T_B(\Delta\lambda)$ values to $\tau_c \leqslant 0.1$ so we could ignore the unknown $\tau_c(T_B)$ relation in equation (3).

The value of the van der Waals coefficient given above is based on a best fit to the observed intensities of the *solar* K wing (White and Suemoto 1968) using the solar photosphere model of Gingerich *et al.* (HSRA, 1971) (see Shine 1973).

The surface gravity we have adopted, $g = 50\ \mathrm{cm\ s^{-2}}$, is consistent with the observed stellar radius ($\sim 23\ R_\odot$) and the probable stellar mass ($\sim 1\ M_\odot$) as taken from Iben's (1967) evolutionary tracks appropriate for a Population II star with $T_{\mathrm{eff}} = 4250 \pm 250$ K (Simon 1970). However, this estimate for the surface gravity may be low by as much as a factor of 2 if Arcturus is actually closer to Population I.

Finally we have adopted a metal abundance deficiency of $[\mathrm{Fe/H}] = -0.50 \pm 0.1$ based on the work of the Griffins (1967; $[\mathrm{Fe/H}] \approx -0.50$), Gustafsson *et al.* (1974; $-0.51 \geq [\mathrm{Fe/H}] \geq -0.61$), and van Paradijs and Meurs (1974; $[\mathrm{Fe/H}] \approx -0.5$). We note that although the above abundance determinations are based on LTE-type analyses, Smith (1974) has shown that departures from LTE in Arcturus's iron spectrum have only minor effects on the derived abundances, at least for unsaturated lines. However, Smith does find that the effects of non-LTE on the equivalent widths of saturated lines causes one to overestimate the photospheric microturbulence parameter by as much as 10 percent using the classical curve of growth analysis. For this reason Smith proposes that the Griffins' (1967) value $\xi_t = 2.2\ \mathrm{km\ s^{-1}}$ should be reduced to $\xi_t = 2.0\ \mathrm{km\ s^{-1}}$, which incidentally is in good agreement with the narrow-band photometry of Gustafsson *et al.* (1974; $\xi_t = 1.7$–$2.1\ \mathrm{km\ s^{-1}}$). Alternatively, Day, Lambert, and Sneden (1973) find a slightly larger velocity $\xi_t = 2.4 \pm 0.14\ \mathrm{km\ s^{-1}}$ from an LTE analysis of the CN red system ($\lambda_0 \approx 8000$ Å), which agrees with the value found by Mount, Ayres, and Linsky (1975; $\xi_t \approx 2.5 \pm 0.2\ \mathrm{km\ s^{-1}}$) based on a *non-LTE* analysis of the CN (0–0) violet system ($\lambda_0 \approx 3883$ Å).

In Figure 4 we have plotted the semiempirical $T_e(m)$ model of Table 1. Also drawn are error bars corresponding to the uncertainties in $T_e$ and $m$ introduced by the uncertainties in the absolute calibration, the gravity, and the metal abundance.

It is clear from Figure 4 that the accuracy of the derived $T_e(m)$ model for Arcturus is limited primarily by errors in the absolute calibration and the metal

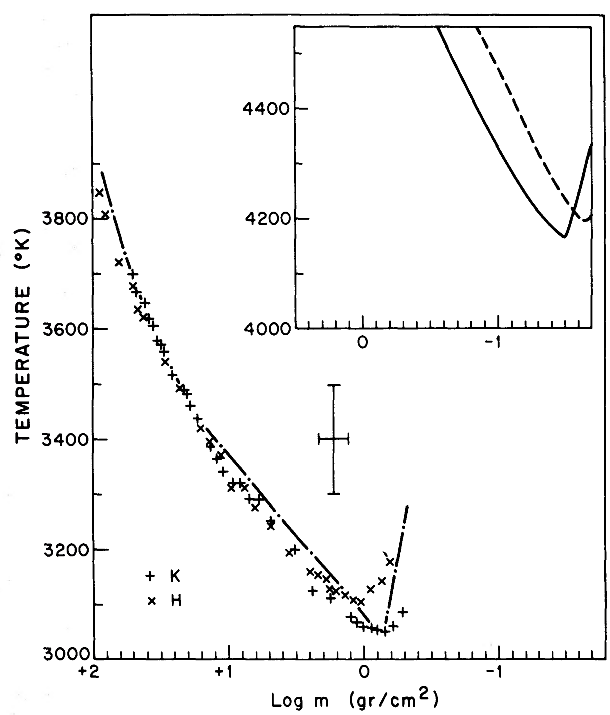


FIG. 4.—Semiempirical $T_e(m)$ model photosphere based on calibrated profiles of H and K. The +'s refer to K line data, and the ×'s to H line data. The dot-dashed curve is the adopted model. For comparison, the temperature minimum regions of two solar models are also plotted: the solid curve is the HSRA (Gingerich *et al.* 1971), and the dashed curve is the model of Mount and Linsky (1974). The vertical error bar refers to the ±100 K uncertainty in the temperature scale attributable to the ±30 percent uncertainty of the absolute calibration; the horizontal error bar refers to the ±0.1 dex uncertainty in the inferred mass scale due to the ±0.1 dex probable error of the calcium abundance measurements.

abundance determination. We note that the value of $T_{\min}$ given here, $T_{\min} \approx T_B(K_1) = 3050 \pm 100$ K, is substantially larger ($\sim 300$ K) than the value quoted in Paper I (Linsky and Ayres 1973) due to an error in the absolute calibration used in Paper I. This correction changes the conclusions of Paper I because we now find that $T_B(K_1)/T_{\text{eff}} \approx 0.74 \pm 0.02$ is essentially identical for the Sun, Procyon, and Arcturus, despite the wide range of gravity and effective temperature spanned by these stars.

Also plotted in Figure 4 for comparison are the HSRA and Mount and Linsky (1974) solar models (temperature minimum regions only). Note that although the temperature structure and mass column density at $T_{\min}$ are slightly different for the two solar models, $m_{T_{\min}}{}^{\odot}$ is clearly much smaller than what we infer for Arcturus. A significant modification to our derived upper-photosphere model based on the effect of partial redistribution (e.g., Milkey, Shine, and Mihalas 1975*b*) on the inner K wing fluxes is discussed in § IV.

### *b) The Model Chromosphere*

#### i) *Comments on the Computational Techniques*

In Paper II we combined a detailed solution of the line-transfer problem for Ca II K (five-level atom + continuum) with a comparatively crude treatment of the hydrogen ionization equilibrium in the atmospheric model. In this paper we replace the analytical approximation used in Paper II to solve for the hydrogen departure coefficients $b_1$ and $b_2$, with an "exact" solution of the Lyman continuum problem based on a two-level + continuum model atom. This approach is a reasonably accurate representation of the ionization equilibrium because to a good approximation L$\alpha$ is in radiative detailed balance in the low and middle solar chromosphere (Noyes and Kalkofen 1970) and probably also in Arcturus's chromosphere. As in Paper II we specify photoionizations from level 2 (the Balmer continuum) using a radiation temperature $T_{R,B}$ which is constant with depth in the chromosphere but equal to the local kinetic temperature in the photosphere for $T_e > T_{R,B}$. The use of a radiation temperature in this fashion to mimic the thermalization properties of the Balmer radiation field is a fairly accurate representation of the true 2-$\kappa$ photoionization rate (see, e.g., Paper IV).

In Paper II we discussed some of the obvious limitations of our single-component, plane-parallel, hydrostatic models. For the Sun and Procyon we argued that the latter two approximations were probably reasonably accurate owing to the high stellar gravities and only mildly asymmetric Ca II K and Mg II *k* profiles. However, for low-gravity stars such as late-type giants and supergiants which also show asymmetric K or *k* profiles, both of these commonly employed assumptions must be considered more closely. For Arcturus, the plane-parallel approximation is probably valid because even though the models we present below are much more geometrically extended than their solar counterparts, the total chromospheric thickness is less than about 10 percent of the stellar radius. Geometrical effects are usually important only where chromospheric extension is comparable to the stellar radius (Kunasz 1973). However, the validity of the hydrostatic assumption is much less clear. Since both *h* and *k* are strongly asymmetric but H and K are not, any large macroscopic velocities must occur near the top of Arcturus's chromosphere where the Ca II lines are optically thin but *h* and *k* are still thick. A perhaps comparable dichotomy is present in the Kondo *et al.* (1972) profiles of *h* and *k* in the M2 supergiant $\alpha$ Ori: *k* shows a strong red-peak enhancement qualitatively similar to that shown by Arcturus's *h* and *k*, but the $\alpha$ Ori *h* line is surprisingly symmetric. Since *k* is only twice as opaque as *h* (*k* is $\sim 7$ times as opaque as K), the onset of large bulk velocities in the $\alpha$ Ori chromosphere must be sharply defined in height; otherwise the *h* profile would be similarly affected. Modisette, Nichols, and Kondo (1973) have proposed an alternative explanation for this curious behavior based on the masking effect of a strong Fe I line in the near short-wavelength wing of the *k* line. The validity of their qualitative explanation should be tested by realistic radiative transfer calculations.

Because H and K are very nearly symmetric ($K_{2v}/K_{2r} \approx H_{2v}/H_{2r} \approx 1.10$), we can be fairly confident that the density structure of Arcturus's chromosphere is close to hydrostatic equilibrium at least over the range of significant K line opacity. However, because the *h* and *k* profiles suggest the existence of large outflow velocities in the upper chromosphere of Arcturus, our static models may not be adequate for *h* and *k*. Furthermore, when significant macroscopic velocity gradients are present in a stellar atmosphere, the assumption of "complete redistribution" in the line transfer solution is probably not adequate to predict accurate source functions for lines such as *k* and K (e.g., Cannon and Vardavas 1974). An explanation of the Arcturus *h* and *k* profiles but based on a better treatment of the redistribution problem in a moving atmosphere is currently being undertaken (Basri and Linsky 1974). For these reasons we base our chromospheric models mainly on the Ca II H and K lines and require only that the computed and measured Mg II fluxes not be inconsistent.

#### ii) *Boundary Conditions: The Temperature Minimum and $P_0$*

In this section we discuss the lower and upper boundaries of a typical stellar chromosphere: the temperature minimum region and the pressure at Lyman continuum optical depth unity, respectively.

We choose the temperature minimum as the lower boundary because it separates two distinct regions of the outer stellar atmosphere: the upper photosphere where the run of temperature with depth is controlled largely by radiative equilibrium, and the chromosphere/corona where the energy balance is likely dominated by nonradiative heating. The temperature minimum, $T_{\min}$, and the location of $T_{\min}$ in "mass" are fixed by the semiempirical upper photosphere model of § III*a*:

$$T_{\min} \approx 3050 \text{ K}; m(T_{\min}) \approx 0.7\text{–}0.8 \text{ g cm}^{-2} .$$

The choice of the "upper boundary condition" for our models, $P_0 \equiv P_{\text{gas}}(\tau_{\text{LyC}} \equiv 1)$, is motivated by the observed behavior of the solar Lyman continuum in quiet and active regions: although the intensities at the head of the Lyman continuum are considerably higher in a typical active region compared with the quiet average, the color temperature of the emission is essentially independent of activity (Noyes and Kalkofen 1970).

Assuming a Lyman continuum source function of the form

$$S_\nu(0) = \frac{B_\nu(T_0)}{b_1(0)} , \quad (6)$$

with

$$T_0 \equiv T_e(\tau_{\text{LyC}} \approx 1) , \quad (7)$$

Noyes and Kalkofen interpret the constancy of $T_{\text{color}}$ as suggesting that the frequency-dependent term in the source function, i.e., $B_\nu(T_0)$, is identical over both active and quiet regions. Since $B_\nu(T_0)$ and therefore $T_0$ are constant, they then attribute the enhanced Lyman continuum intensities in active regions solely to the effect of the increased upper chromospheres pressures $P_0$ on the "surface value" of the departure coefficient, $b_1(0)$ (see also Shine and Linsky 1974*b*). Hence, even though $P_0$ may change significantly from star to star, we expect $T_0 \approx 8 \times 10^3$ K to remain relatively independent of $P_0$ as is observed over a wide range of chromospheric pressures on the Sun.

We exploit this physical simplification to construct a grid of model chromospheres for Arcturus based on linear (in $\log m$) temperature rises from the fixed lower boundary $[T_{\min}, m(T_{\min})]$ up to $(T_0, m_0 = P_0/g)$. Above $(T_0, m_0)$ the model temperatures increase exponentially to $T_e = 10^4$ K to mimic the effect of the onset of a steep transition region (TR) temperature gradient. The requirement of a sharp chromospheric temperature rise above $\tau_{\text{LyC}} \approx 1$ is discussed by Thomas and Athay (1961), Defouw (1970), Vernazza, Avrett, and Loeser (1973), and others. We choose $T_e = 10^4$ K as the upper cutoff temperature for our models because, owing to ionization, there is a negligible contribution to $\tau_k$ or $\tau_K$ from the stellar upper chromosphere ($T_e > 10^4$ K), transition region, and corona. Using such a grid, we can compute the Ca II and Mg II emission as a function of $P_0$. In this way we can hope to set fairly reliable limits on the upper boundary pressure of Arcturus's chromosphere based on the observed Ca II and Mg II emission and thereby estimate limits on the strength of TR or coronal emission lines accessible from satellite- or rocket-borne spectrometers.

iii) *The Microvelocity Model*

In complete redistribution limit the profile of the K-line core (or equivalently the integrated flux) is sensitive to basically two gradients: temperature and microvelocity. Physically, increasing the temperature gradient (1) increases ionization of the metals and hydrogen, thereby increasing $\epsilon \equiv n_e\Omega_{ul}/A_{ul}$ (e.g., Linsky and Avrett 1970) which forces the K line to thermalize higher in the atmosphere and therefore at a higher temperature and (2) increases the chromospheric Planck function at each optical depth (cf. Shine and Linsky 1974*b*), hence forcing the thermalized portions of the line source function to higher values. Both effects tend to increase the core flux. The effect of increasing the microvelocity gradient on the line profiles, other than the obvious broadening of the core, is more subtle. However, for both the Sun and Procyon—and for complete redistribution—we find that changes in the temperature gradient have a greater effect on the emergent K line flux than do changes in the microvelocities, at least within the limits imposed on the $\xi_t(m)$ distribution by the requirement of fitting the wavelengths of the $K_2$ peaks (see, e.g., Paper II).

For this reason, and for the sake of simplicity, we consider only constant gradient $[d\xi_t(m)/d \log m]$ microvelocity models; $\xi_t$ = const. = 2 km s$^{-1}$ in the stellar photosphere, and $\xi_t$ increasing linearly in $\log m$ from $\xi_t = 2$ km s$^{-1}$ at $T_{\min}$ to $\xi_t = \xi_t^{(0)} \approx 10$ km s$^{-1}$ at $T_0$ in the chromosphere. The choice of this particular range of $\xi_t(m)$ models is not completely arbitrary because the measured photospheric microvelocities for Arcturus are on the order of 2 km s$^{-1}$ (see, e.g., § III*a*) and $\xi_t^{(0)} = 10$ km s$^{-1}$ is on the order of the sound speed at $T_0$: we would not expect to find a much larger value of $\xi_t^{(0)}$ because the "turbulent eddies" characterized by $\xi_t$ would then dissipate very rapidly due to shock wave formation. The $\xi_t(m) = (2, 10)$ microvelocity model is qualitatively similar to those proposed for the solar chromosphere by Linsky and Avrett (1970) and Vernazza *et al.* (1973) and for Procyon in Paper II.

iv) *Atomic Models*

Our non–LTE radiative transfer/statistical equilibrium calculations for Arcturus are based on a version of the code PANDORA (Vernazza *et al.* 1973) with a five-level representation of the $Ca^+$ ion (e.g., Linsky and Avrett 1970) and a two-level representation of $Mg^+$ (e.g., Dumont 1967). The model $Ca^+$ ion consists of the $4s\,^2S$ ground state and the doublet $4p\,^2P$ and $3d\,^2D$ excited states. The less complex $Mg^+$ model consists of the $3s\,^2S$ ground state and the higher lying of the doublet $3p\,^2P$ excited states (i.e., $3p\,^2P_{3/2}$, the upper level of the $k$ line). In addition we include the $Ca^{++}$ and $Mg^{++}$ ionization continua, and treat the neutral fractions $Ca/Ca^+$ and $Mg/Mg^+$ in LTE. The collisional excitation and ionization rates and photoionization cross sections for both $Ca^+$ and $Mg^+$ are taken from Shine and Linsky (1974*b*) and Shine (1973). The photoionization rates, themselves, are based on the measured integrated flux of the Arcturus L$\alpha$ line ($Ca^+$ $4p$, $3d$ only), and a rough estimate of the Lyman continuum intensities from preliminary model chromospheres calculations.

TABLE 2

INTEGRATED FLUXES $\pi F$ (ergs cm$^{-2}$ s$^{-1}$) FOR A GRID OF MODEL CHROMOSPHERES

| $\log m_0$ (g cm$^{-2}$) | | $\xi_t$ (km s$^{-1}$) (2, 7.5) | (2, 12.5) | (2, 15.0) |
|---|---|---|---|---|
| $-3.5$ ........... | $K_{calc}$ | 1.06(5) | 1.02(5) | |
| | $H_{calc}$ | | 9.41(4) | |
| | $k_{calc}$ | | 2.89(5) | |
| $-4.0$ ........... | $K_{calc}$ | 8.41(4) | 8.51(4)* | 8.35(4) |
| | $H_{calc}$ | | 8.08(4) | |
| | $k_{calc}$ | 1.08(5) | 1.05(5) | 1.04(5) |
| $-4.5$ ........... | $K_{calc}$ | | 5.66(4) | 5.55(4) |
| | $H_{calc}$ | | 4.19(4) | |
| | $k_{calc}$ | | 5.75(4) | |
| | $K_{obs}$ | | 6.8(4) ± 30% | |
| | $H_{obs}$ | | 6.7(4) ± 20% | |
| | $k_{obs}$ | | 1.1(5) ± 50% | |

* $K_{calc}$ = 8.19(4) for 2 × (4$p$, 3$d$) photo rates, = 1.02(5) for 1/2 × (4$p$, 3$d$) photo rates.

We find that the Ca II H and K lines are somewhat sensitive to these photoionization rates, particularly the rates out of the 4$p$ and 3$d$ levels which are dominated by a strong L$\alpha$ background [$\pi F_{L\alpha}(\alpha$ Boo) $\approx$ 0.1–0.2 × $\pi F_{L\alpha}(\odot)$: Moos and Rottman 1972, Linsky *et al.* 1974]. We also find that the Mg II $k$ line is relatively insensitive to the 3$s$ and 3$p$ photoionization rates which are dominated by a weak Lyman continuum [$\pi F_{LyC}(\alpha$ Boo) $\approx 0.02 - 0.04 \times \pi F_{LyC}(\odot)$; based on a comparison of Lyman continuum intensities for a range of Arcturus and solar chromosphere models; see Paper IV]. Fortunately, the uncertainty in the H and K integrated fluxes introduced by the roughly ±50 percent uncertainty in the measured L$\alpha$ flux has a minor effect on inferring a model chromosphere.

### v) *A Grid of Model Chromospheres*

The results of our multilevel complete redistribution profile synthesis for the Ca II and Mg II emission cores are summarized in Table 2 and Figure 5 which give the integrated fluxes in H, K, and $k$ as functions of $m_0$, $\xi_t$, and the (4$p$, 3$d$) photoionization rates. From Figure 5 we see that only a narrow range of $m_0$—or equivalently $P_0$—is consistent with the observed fluxes of the Ca II and Mg II lines within the experimental error attached to each set of observations:

$$-4.0 < \log m_0 < -4.5 \,. \tag{8}$$

As one might expect, the Mg II $k$ line is a more sensitive indicator of $m_0$ than the Ca II lines, although in practice the larger uncertainty in the absolute calibration of $k$, and the possibly significant effect of

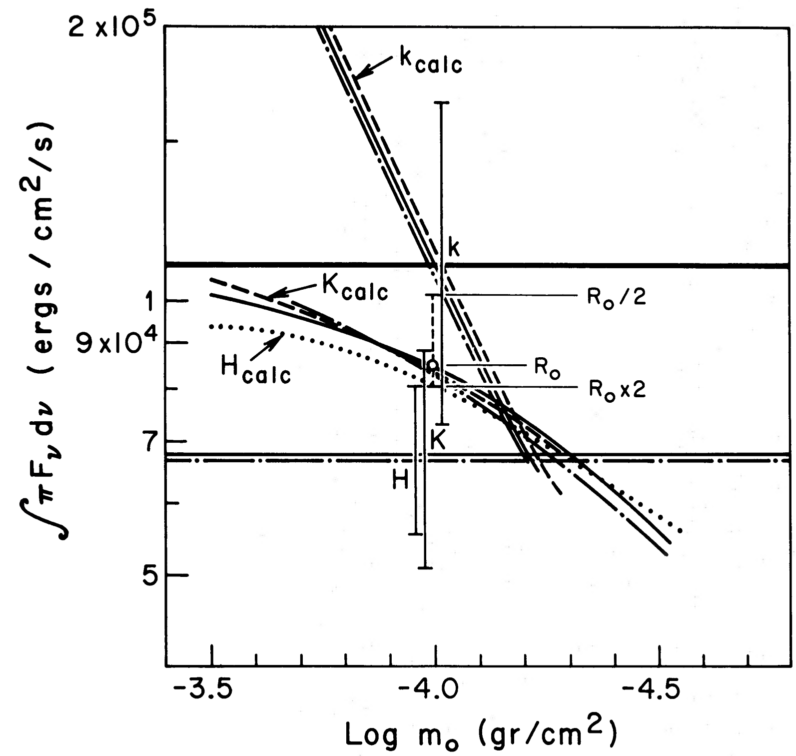


FIG. 5.—Computed fluxes of Ca II H and K and Mg II $k$ as functions of $\log m_0$ for several $\xi_t$ models. The integration bandpass $\Delta\lambda_0$ is ±0.75 Å for H and K and ±1.00 Å for $k$. The horizontal lines refer to the observed integrated fluxes, and the vertical error bars are the calibration uncertainties. The plotted $K_{calc}$ and $k_{calc}$ curves include the three microvelocity models $\xi_t$ = (2, 7.5) (– – – –); $\xi_t$ = (2, 12.5) (———); and $\xi_t$ = (2, 15.0) (–·–·–·–). $H_{calc}$ (––––) is plotted for the $\xi_t$ = (2, 12.5) model only. The vertical dashed error bar illustrates the uncertainty in $K_{calc}$ introduced by a factor of 2 uncertainty in the (4$p$, 3$d$) photoionization rates $R_0$.

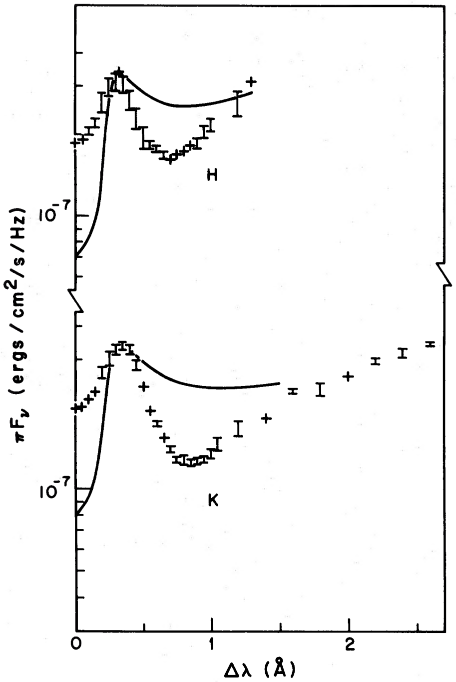


FIG. 6a

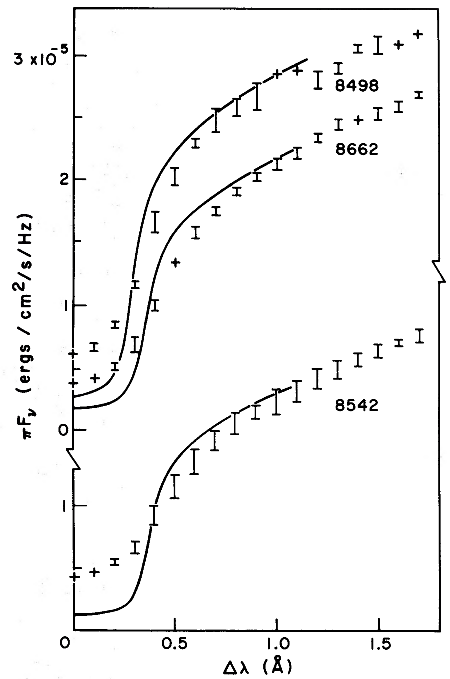


FIG. 6b

FIG. 6a.—Synthesized complete redistribution profiles of Ca II H and K for $\log m_0 = -4.0$, $\xi_t = (2, 12.5)$, and the nominal ($4p$, $3d$) photoionization rates.

FIG. 6b.—Synthesized infrared triplet profiles for the model described in Fig. 6a.

velocity fields on the $k$ emission, tend to nullify this advantage. We also point out the variation of $K_{calc}/H_{calc}$ with $m_0$ for the fixed $\pm 0.75$ Å bandpass. This ratio decreases with decreasing $m_0$, crossing unity at $\log m_0 = -4.3$. Interestingly the $\log m_0 = -4.3$ model not only reproduces the absolute flux of both H and K within the calibration uncertainty, but also the flux ratio, which has a much smaller probable error than the absolute calibration itself. We caution, however, that because our calculations are based on complete redistribution rather than partial redistribution (see, e.g., § IV) the coincidence of $K_{calc}$ and $K_{calc}/H_{calc}$ with the observed quantities at $\log m_0 = -4.3$ may be fortuitous.

As indicated by Figure 5, the core fluxes of Ca II K and Mg II $k$ are more sensitive to the surface pressure $P_0$ than to the microvelocity model $\xi_t$. In fact, as mentioned above, severe limits on the possible microvelocity models are dictated by the requirement of fitting the $K_2$ emission peak wavelengths. Conversely, we find that the infrared triplet profiles are much more sensitive to the microvelocity models than to $P_0$. Interestingly the microvelocity model $\xi_t = (2, 12.5)$, in the notation of § III*b*(iii) above, produces the best fit to *both* the $K_2$ wavelength and the subordinate line cores. The H, K, and infrared triplet profiles synthesized for the $\xi_t = (2, 12.5)$ microvelocity model, the $\log m_0 = -4.0$ temperature distribution, and the nominal ($4p$, $3d$) photoionization rates are illustrated in Figure 6. We note that a much improved fit to the $H_3$ and $K_3$ features for the $\log m_0 = -4.0$ model results from decreasing the nominal photoionization rates by about 50 percent, which would not be inconsistent with the experimental error attached to the Arcturus Lα measurement. Furthermore, a much improved fit to the infrared triplet could be accomplished by smearing the synthesized profiles with a Gaussian *macrovelocity* of $\sim 10$ km s$^{-1}$ (e.g., Paper II) or by invoking the "mesoturbulence" hypothesis of Shine and Oster (1973). Either broadening mechanism might be expected to significantly raise the core intensities.

#### vi) *The Effect of Gravity and Metal Abundance on the Inferred Model*

In order to test the possible influence of $g$ and $A_{Ca}$ we constructed a set of models having either enhanced gravity or metal abundance. We found that a factor of 2 error in $g$ corresponds to only about a two-tenths of a dex uncertainty in $\log m_0$, and that the one-tenth dex uncertainty in the adopted value of $A_{Ca}$ corresponds to only a tenth dex error in $\log m_0$. Both of these uncertainties are comparable to that introduced by the roughly $\pm 30$ percent uncertainty in the absolute calibration of the K line.

From the above considerations we see that the chromospheric model (i.e., $P_0$) is reasonably well determined—in the complete redistribution limit—despite uncertainties in the fundamental stellar parameters.

IV. THE EFFECTS OF PARTIAL REDISTRIBUTION

Considerable progress has been made recently toward understanding the effects of partial frequency redistribution on the source functions of strong resonance lines. An excellent discussion of the physical and numerical aspects of partial redistribution (PRD) is given by Milkey and Mihalas (1973*a*) and Milkey *et al.* (1975*b*). These PRD techniques are applied to the solar L$\alpha$ and Mg II *h* and *k* lines by Milkey and Mihalas (1973*b*, 1974), to the *h* and *k* lines in solar-type stars of varying gravity by Milkey *et al.* (1975*a*), and to the solar Ca II H and K lines by Shine, Milkey, and Mihalas (1975).

The preliminary studies based on the Mg II *h* and *k* and Ca II H and K lines have demonstrated that the inner wing intensities near the $H_1$ and $K_1$ features are particularly sensitive to PRD effects, primarily because the frequency-dependent inner wing source functions become uncoupled from the saturated core source functions. In fact, beyond the Doppler core, the monochromatic wing source functions begin to assume the character of coherent scattering solutions modified by a depth-dependent fraction of incoherence produced by pressure broadening effects. In the case of Ca II, further incoherence is introduced by subordinate radiative transitions (Milkey *et al.* 1975*b*).

Because the effects of PRD are likely to be large at the low densities of Arcturus's upper photosphere, we have applied the PRD approach to the Arcturus K line in an effort to estimate possible departures from the complete redistribution (CRD) approximation used in § III above, and the effect of such departures on the inferred upper photosphere $T_e(m)$ model.

*a*) *Numerical Techniques*

For simplicity and numerical tractability we base our solution of the PRD radiative transfer problem on a code written by R. A. Shine for a two-level representation of Ca II. We have modified this code to crudely account for the presence of the Ca II metastable states by including a fixed percentage ($\sim 6\%$) of complete redistribution to mimic the fraction of noncoherence attributable to the infrared triplet, and correcting the K-line optical depth scale for the LTE population of the 3*d* states. This latter approximation should be adequate for the photospheric wings of the K line. We generate the $R^{\rm II}$ weights (e.g., Hummer 1968) by interpolating between two tables utilizing essentially a Taylor expansion in the Voigt parameter, thus realizing a considerable savings in computer time over previous methods (e.g., Adams, Hummer, and Rybicki 1971). We note that the wing intensities predicted by the modified code—in particular $I_{K_1}$—agree very well with the numerically much more elaborate five-level calculation (e.g., Shine *et al.* 1975) for the HSRA (Gingerich *et al.* 1971) solar model.

In Figure 7 we plot inner wing profiles of Ca II K in both the CRD and PRD approximations based on the upper photosphere model of § III. It is clear from this figure that departures from CRD in Arcturus are substantial. Such departures are to be expected for low-density atmospheres owing to the weakened effect of pressure broadening (see also Milkey *et al.* 1975*a*), although the departures are less for Ca II K than for Mg II *k* owing to the lower bound on the K line incoherence fraction (Milkey *et al.* 1975*b*) provided by the infrared triplet. Qualitatively, the effect of PRD is to lower the inner wing intensities and to shift the $K_1$ minimum somewhat closer to line center compared with the CRD result. Also note that the shape of the PRD profile is in better qualitative agreement with the observed K wing fluxes: it is difficult to produce the steep $K_2$–$K_1$ intensity gradient with a frequency independent source function (i.e., CRD), but a sharp $K_2$–$K_1$ transition appears to be a simple consequence of PRD. Interestingly, previous explanations of the Wilson-Bappu effects have assumed that the steep $K_2$–$K_1$ intensity gradient common in stellar K line profiles could result only from a Doppler-broadened emission core (Wilson 1966, 1972; Reimers 1973). However, in the framework of PRD, a sharp transition between $K_2$ and $K_1$ can also be produced by the radiation-damping–dominated inner wings of K simply by having a steep chromospheric temperature rise.

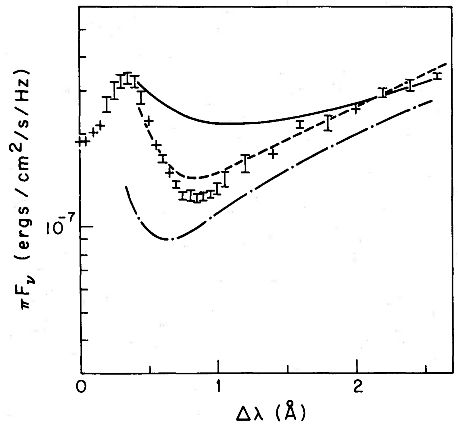


FIG. 7.—Complete redistribution approximation compared with partial redistribution. The solid curve is the inner wing profile of the K line based on CRD and the upper photosphere model of § III (e.g., Fig. 4). The dot-dashed curve is the PRD wing profile for the same model atmosphere. The dashed curve is a two-level PRD K-line profile for the modified upper photosphere model of Fig. 8.

In Figure 7 we illustrate a two-level approximation PRD K line profile synthesized for the modified upper photosphere/low chromosphere model of Figure 8 ("PRD"). We have adopted $T_{\rm min} = 3200$ K,

$$\log m(T_{\rm min}) = 0.25 \text{ g cm}^{-2} ,$$

and the standard velocity model of § III to produce a reasonable fit to the observed inner wings, $K_1$ features, and the initial rise to the $K_2$ emission peaks.

*b*) *The Adopted Model*

In the previous section we found significant departures from the CRD solution for the inner wings

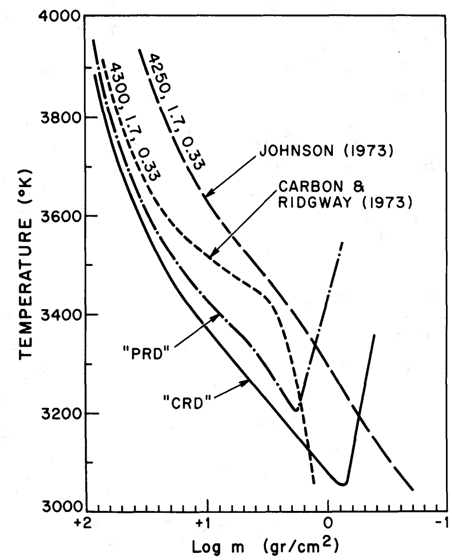


FIG. 8.—Upper photosphere models: solid curve is the $T_e(m)$ distribution inferred from the H and K wings assuming CRD (e.g., § III), while the dot-dashed curve is the PRD modified upper photosphere model. The theoretical, line blanketed, RE models of Carbon and Ridgway (1973, – – –) and Johnson (1973, ——— ———) are plotted for comparison.

of the K line, especially near the $K_1$ minimum features. However, the emission core ($K_2$–$K_3$–$K_2$) is much less sensitive to the differences between CRD and PRD, basically because complete redistribution is a good approximation for the Doppler-dominated portion of the line profile (see Shine *et al.* 1975). Moreover, at present it is not feasible to carry out the numerically formidable five-level PRD calculation for a grid of model chromospheres comparable to that of § III, although we do contemplate such a study using a less accurate but more tractable three-level PRD calculation (Paper V). We therefore propose a preliminary upper photosphere/low chromosphere model for Arcturus based on the PRD upper photosphere of the previous section with $T_{\rm min} = 3200$ K and $\log m(T_{\rm min}) = 0.25$ g cm$^{-2}$ and a CRD-type linear (in $\log m$) temperature rise in the chromosphere consistent with the range of $T_e(m)$ models suggested by the calculations of § III. We note that there is a certain ambiguity introduced by this hybridization scheme in that the CRD calculations of § III are based on a $T_{\rm min}{}^{\rm CRD}$ approximation 5 percent lower and a $\log m^{\rm CRD}(T_{\rm min})$ 0.4 dex smaller than what we have adopted for the final model. However, we can compensate for the higher PRD temperatures in the vicinity of $T_{\rm min}$ by using a slightly flatter chromospheric temperature rise (i.e., smaller $m_0$) in order to achieve comparable temperatures near the $K_2$ source function maximum. Since the $K_2$–$K_3$–$K_2$ intensities are sensitive primarily to the temperature-density structure of the middle chromosphere above the temperature minimum, the flatter PRD $T_e(m)$ model should give essentially the same core flux as the corresponding CRD model. We find that the range of $m_0{}^{\rm PRD}$,

$$-4.5 \geq \log m_0{}^{\rm PRD} \geq -5.0\,, \tag{9}$$

gives a satisfactory correspondence to the range of $m_0{}^{\rm CRD}$ given in § III.

The number densities for the adopted model (with $\log m_0 = -4.5$) are tabulated in Table 3 and plotted

TABLE 3

ADOPTED MODEL

| $m$ (g cm$^{-2}$) | $T_e$ (K) | $P_e$ (dyn cm$^{-2}$) | $n_{\rm H\,I}$ (cm$^{-3}$) | $b_1$ | $b_2$ |
|---|---|---|---|---|---|
| 1. 3.0818(−5) | 10000 | 5.574(−4) | 2.437(8) | 5.140(5) | 1.656(4) |
| 2. 3.0823(−5) | 9457 | 5.042(−4) | 3.357(8) | 2.883(5) | 1.054(4) |
| 3. 3.0969(−5) | 8459 | 4.640(−4) | 4.466(8) | 4.282(4) | 3.780(3) |
| 4. 3.1623(−5) | 8000 | 5.221(−4) | 3.989(8) | 8.532(3) | 2.348(3) |
| 5. 3.5604(−5) | 7948 | 6.704(−4) | 3.083(8) | 3.436(3) | 2.159(3) |
| 6. 4.7472(−5) | 7822 | 8.772(−4) | 4.471(8) | 1.998(3) | 1.931(3) |
| 7. 7.1434(−5) | 7642 | 1.118(−3) | 1.055(9) | 1.669(3) | 1.677(3) |
| 8. 1.3162(−4) | 7374 | 1.408(−3) | 3.236(9) | 1.345(3) | 1.346(3) |
| 9. 2.8281(−4) | 7038 | 1.596(−3) | 1.009(10) | 1.000(3) | 1.001(3) |
| 10. 6.6258(−4) | 6665 | 1.586(−3) | 2.944(10) | 6.965(2) | 6.967(2) |
| 11. 1.6165(−3) | 6273 | 1.407(−3) | 8.172(10) | 4.563(2) | 4.565(2) |
| 12. 4.0127(−3) | 5874 | 1.132(−3) | 2.222(11) | 2.807(2) | 2.808(2) |
| 13. 1.0032(−2) | 5472 | 8.331(−4) | 6.014(11) | 1.607(2) | |
| 14. 2.5151(−2) | 5069 | 5.837(−4) | 1.632(12) | 8.445(1) | |
| 15. 6.3127(−2) | 4665 | 4.218(−4) | 4.453(12) | 3.988(1) | |
| 16. 1.5852(−1) | 4261 | 3.227(−4) | 1.224(13) | 1.644(1) | |
| 17. 3.9814(−1) | 3857 | 5.533(−4) | 3.398(13) | 5.679(0) | |
| 18. 1.0000(0) | 3453 | 9.098(−4) | 9.533(13) | 1.546(0) | |
| 19. 1.7783(0) | 3200 | 7.532(−4) | 1.829(14) | 5.839(−1) | |
| 20. 2.5119(0) | 3250 | 1.109(−3) | 2.544(14) | 7.162(−1) | |
| 21. 3.9811(0) | 3330 | 1.918(−3) | 3.935(14) | 9.810(−1) | |
| 22. 6.3096(0) | 3375 | 2.975(−3) | 6.153(14) | 1.000 | |
| 23. 1.2589(+1) | 3460 | 5.990(−3) | 1.198(15) | 1.000 | |
| 24. 1.9953(+1) | 3530 | 9.829(−3) | 1.860(15) | 1.000 | |
| 25. 3.1623(+1) | 3620 | 1.679(−2) | 2.875(15) | 1.000 | |
| 26. 5.0119(+1) | 3735 | 2.992(−2) | 4.417(15) | 1.000 | |
| 27. 7.9433(+1) | 3935 | 6.067(−2) | 6.644(15) | 1.000 | |

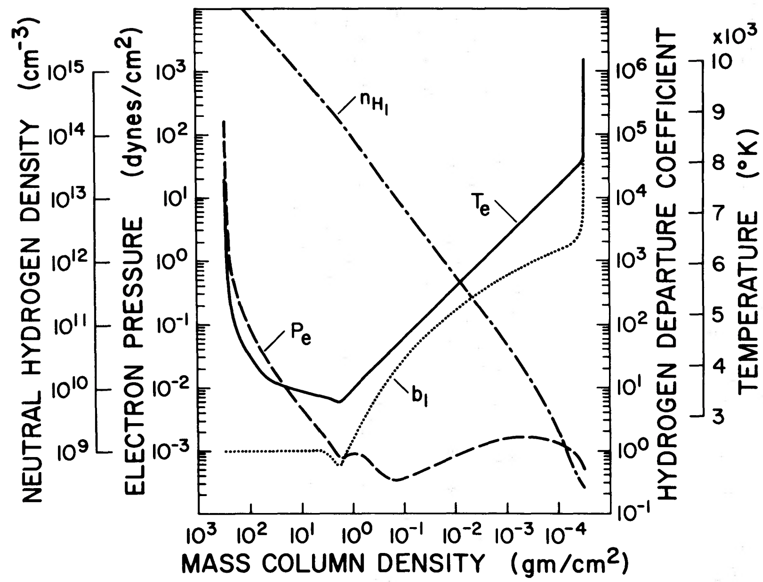


FIG. 9.—Number densities for the adopted model: $T_{\min} = 3200$ K, $\log m(T_{\min}) = 0.25$ g cm$^{-2}$; $T_0 = 8000$ K, $\log m_0 = -4.5$ g cm$^{-2}$.

in Figure 9. The hydrogen ionization equilibrium calculation is based on a Balmer radiation temperature of $T_{R,B} = 3340 \pm 100$ K estimated from Willstrop's (1965) ultraviolet fluxes ($\lambda < 3650$ Å).

## V. DISCUSSION

We have presented above a simple model for the upper photosphere and low chromosphere of Arcturus, consistent with the observed emission cores of Ca II H and K and Mg II *k* and the Ca II H and K wings. A more detailed model could be devised, but we feel that such an approach is not justifiable until we have a reliable estimate of the extent to which our assumptions of a homogeneous, static, plane-parallel chromosphere are valid for Arcturus and have a better understanding of the effects of partial frequency redistribution on the emission cores of K and *k*.

Despite the simplicity of our Arcturus model compared with solar models, we can draw several conclusions concerning the outer atmospheres of Arcturus and similar stars.

1. The effects of partial redistribution on the inner wings of both Ca II H and K and Mg II *h* and *k* in Arcturus are substantial. The modifications to the CRD-based upper photosphere model of § III required to fit the observed K wing in the PRD limit are: $\Delta T \approx +150$ K near $T_{\min}$ and $\Delta \log m(T_{\min}) \approx 0.4$

TABLE 4

COMPARISON OF THREE STARS

| | STAR | | |
|---|---|---|---|
| PARAMETER | Sun | Procyon | Arcturus |
| Spectral type | G2 V | F5 IV–V | K2 IIIp |
| $T_{\rm eff}$ [K] | 5770 ± 10 | 6420 ± 65 | 4250 ± 100 |
| Gravity [cm s$^{-2}$] | $2.74 \times 10^4$ | $1.0 \times 10^4$ | $5.0 \times 10^1$ |
| $T_B(K_{1V})$ [K] | 4280 ± 80 | 4850 ± 100 | 3050 ± 100 |
| $T_{\min}^{\rm CRD}$ [K] | 4170 | 4750 | 3050 |
| $T_{\min}^{\rm PRD}$ [K] | 4470 | 5080 | 3200 |
| $\Delta T \equiv T_B - T_{\min}^{\rm PRD}$ | 190 | 230 | 150 |
| $T_{\min}^{\rm PRD}/T_{\rm eff}$ | 0.775 ± 0.014 | 0.791 ± 0.023 | 0.753 ± 0.018 |
| $m^{\rm CRD}(T_{\min})$ [g cm$^{-2}$] | 0.032 | 0.063 | 0.75 |
| $m^{\rm PRD}(T_{\min})$ [g cm$^{-2}$] | 0.06–0.03 | ~0.11 | 1.8 |
| $T_0$ [K] | 8300 | 8000 | 8000 |
| $m_0$ [g cm$^{-2}$] | $5.5 \times 10^{-6}$ | $5.5 \times 10^{-6}$ | $3 \times 10^{-5}$ |
| $P_0 = m_0 g$ [dyn cm$^{-2}$] | 0.15 | 0.055 | 0.0015 |
| $A_{el}P_0^2/g$ | $8.2 \times 10^{-7}$ | $3.0 \times 10^{-7}$ | $1.5 \times 10^{-8}$ |
| $A_{el}P_0/[A_{el}P_0]_\odot$ | 1.00 | 0.37 | 0.003 |
| $[A_{el}P_0^2/g]/[A_{el}P_0^2/g]_\odot$ | 1.00 | 0.37 | 0.018 |

(e.g., Fig. 8). However, despite the PRD modifications, it appears that the ratio $T_{\min}/T_{\text{eff}}$ may be similar for a wide variety of late-type stars as suggested in Paper I of this series, but larger than the value $0.74 \pm 0.02$ given by the observed $T_B(\text{K}_1)/T_{\text{eff}}$ ratios. Included in Table 4 are the values of $T_{\min}^{\text{CRD}}$ for the Sun (Linsky and Avrett 1970), Procyon (Paper II), and Arcturus (§ III) and for comparison purposes $T_B(\text{K}_{1\text{V}})$ for the three stars corrected for the calibration errors in Arcturus and Procyon (see Paper II). We include the value of $T_{\min}^{\text{PRD}}$ for Arcturus estimated in § IV and values of $T_{\min}^{\text{PRD}}$ for the Sun (4470 K) and Procyon (5080 K) estimated in the same manner. The solar value of $T_{\min}^{\text{PRD}}$ is similar to the value 4450 K suggested by Shine *et al.* (1975). Notice that $\Delta T = T_{\min}^{\text{PRD}} - T_B(\text{K}_{1\text{V}})$ increases slowly from Arcturus → Sun → Procyon and $T_{\min}^{\text{PRD}}/T_{\text{eff}} \approx 0.77$ for all stars within the estimated errors, suggesting the possibility that this ratio may be similar for all F–K stars of luminosity classes III–V.

2. The long-standing explanation of the Wilson-Bappu effect (see, e.g., Wilson 1966) based on a presumed correlation of chromospheric microvelocity with luminosity may not be correct: we find instead that the velocity models consistent with the $\text{K}_2$ widths of Procyon, the Sun, and Arcturus (with complete redistribution) are very similar despite the wide range of luminosities represented by these three stars. Furthermore, PRD suggests that the K-line emission width, $W_0$, may be controlled by the damping wing rather than the Doppler core. A more likely explanation for the width-luminosity relation obeyed by both the core and damping wings of Ca II H and K (also Mg II *h* and *k*; Kondo *et al.* 1972) lies in the systematic increase in photospheric mass column density encountered (see Table 4) going from high gravity (i.e., low luminosity) to low gravity (i.e., high luminosity) stars due to the quadratic pressure sensitivity of $\text{H}^-$ formation (Ayres *et al.* 1975). This problem is currently being investigated within the context of PRD for realistic stellar models and will be discussed in detail in a subsequent paper of this series (Paper V).

3. We estimate that at the top of the chromosphere $T_0 \approx 8000$ K, $\log m_0 = -4.5$, and $P_0 = m_0 g = 1.5 \times 10^{-3}$ dyn cm$^{-2}$. The chromospheric boundary pressure is thus about 1 percent of the solar value of 0.15 dyn cm$^{-2}$ (Dupree 1972). If $m_0 = 10^{-5.0}$, the probable minimum value of $m_0$ consistent with our analysis, then $P_0$ is only 0.003 of the solar value. If $T_0$ is substantially smaller than 8000 K, then $m_0$ may be somewhat larger than $10^{-4.5}$. As noted in Table 4, there is a trend of decreasing $P_0$ in the sequence Sun → Procyon → Arcturus corresponding to decreasing gravity even though $m_0$ is larger in Arcturus than in the Sun. In the Sun the transition region (TR) is less than a pressure scale height thick due to the inability of the solar plasma to radiate sufficient energy to balance nonradiative heating terms in the temperature region $10^4$–$10^6$ K. The result is a narrow TR in which, for the most part, the divergence of the conductive flux is balanced by radiative losses. By analogy it seems reasonable to expect that the TR is narrow for Arcturus and other late-type stars as indeed Ulmschneider (1967) and Kuperus (1965) compute; hence it is likely that the value of $P_0$ in the upper chromosphere also represents the pressure throughout the stellar TR and at the base of the stellar corona. Given that the strength of the spectrum of a collisionally excited TR ion scales as $\sim A_{el}P_0^2(dT/dz)^{-1}$, where $A_{el}$ is the atomic abundance, and that the temperature gradient quite likely is proportional to $P_0$ (Gerola *et al.* 1974), we can estimate from the inferred value of $P_0$ (§ IV) that optically thin lines in Arcturus's TR should have less than 1 percent the surface brightness of corresponding solar lines. Upper limits on the surface brightness of the Si III λ1206 line (Linsky *et al.* 1975) are consistent with this result. Optically thick lines such as Lα, He I λ584, and He II λ304, formed at the base of the TR where the energy balance and temperature gradient may be much different, need not be so faint. In particular, the surface brightness of the Arcturus Lα line uncorrected for interstellar absorption is one-quarter that of the Sun (Moos and Rottman 1972) or 0.13 that of the Sun as determined by Linsky *et al.* (1975).

Similarly, the strength of coronal line radiation is proportional to $A_{el}P_0^2/g$ for those ions abundant at the coronal temperature $T_{\text{cor}}$, assuming collisional excitation, isothermal, and hydrostatic equilibrium conditions (Gerola *et al.* 1974). Thus if $T_{\text{cor}}$ is similar in Arcturus and the Sun, we would expect the surface brightness of coronal lines to be about 2 percent of their solar values. Recently the O V λ1218 line has been observed in the K0 giant β Gem (Gerola *et al.* 1974), suggesting $T_{\text{cor}}$ near 260,000 K for that star. However, the O V line has not been observed in Arcturus (Linsky *et al.* 1975), implying that $T_{\text{cor}}$ for Arcturus is either much larger or much smaller than 260,000 K.

Ulmschneider (1967) and Kuperus (1965) have proposed that the acoustic flux heating of the outer atmospheres of late-type stars should increase with decreasing gravity. We see no evidence that this is true since the surface brightness of chromospheric, TR, and probably also coronal lines are much less than for the Sun. However, Arcturus does appear to have a large stellar wind (Linsky *et al.* 1974; Basri and Linsky 1974) which may carry out most of the nonradiative energy input to its outer atmosphere.

4. We have demonstrated that our model building techniques are feasible for an evolved, metal-deficient star of late spectral type and low surface gravity. For this reason we expect our approach to be reasonably valid for most "normal" late-type stars in luminosity classes III–V.

We acknowledge support of the National Aeronautics and Space Administration through grants NAS5-23274 and NGR-06-003-057 to the University of Colorado. We also wish to thank R. Shine, H. Gerola, and G. Mount for helpful discussions.

## REFERENCES

Adams, T. F., Hummer, D. G., and Rybicki, G. B. 1971, *J. Quant. Spectrosc. and Rad. Transf.*, **11**, 1362.
Ayres, T. R. 1975, *Ap. J.* (in press).
Ayres, T. R., and Linsky, J. L. 1975*a*, *Ap. J.* (in press). (Paper IV.)
———. 1975*b* (in preparation, Paper V).
Ayres, T. R., Linsky, J. L., and Shine, R. A. 1974, *Ap. J.*, **192**, 92 (Paper II).
———. 1975, *Ap. J.* (*Letters*), **195**, L121.
Ayres, T. R., Linsky, J. L., Shine, R. A., and Chipman, E. 1973, *Bull. AAS*, **5**, 364.
Basri, G. S., and Linsky, J. L. 1974 (in preparation).
Brinkmann, R. T., Green, A. E. S., and Barth, C. A. 1966, Tech. Rept. No. 32–951, Jet Propulsion Lab.
Cannon, C. J., and Vardavas, I. M. 1974, *Astr. and Ap.*, **32**, 85.
Carbon, D. F., and Ridgway, S. 1973 (unpublished).
Cayrel, R. 1963, *Comp. Rend. Acad. Sci. Paris*, **257**, 3309.
Conti, P. S., Greenstein, J. L., Spinrad, H., Wallerstein, G., and Vardya, M. S. 1967, *Ap. J.*, **148**, 105.
Day, R. W., Lambert, D. L., and Sneden C. 1973, *Ap. J.*, **185**, 213.
Defouw, R. J. 1970, *Solar Phys.*, **14**, 42.
Doherty, L. R. 1972, *Ap. J.*, **178**, 495.
Dumont, S. 1967, *Ann. d'Ap.*, **30**, 861.
Dupree, A. K. 1972, *Ap. J.*, **178**, 527.
Fosbury, R. A. E. 1973, *Astr. and Ap.*, **27**, 129.
Gerola, H., Linsky, J. L., Shine, R., McClintock, W., Henry, R. C., and Moos, H. W. 1974, *Ap. J.* (*Letters*), **193**, L107.
Gingerich, O., Noyes, R. W., Kalkofen, W., and Cuny, Y. 1971, *Solar Phys.*, **18**, 347.
Greene, T. F. 1969, *Ap. J.*, **157**, 737.
Griffin, R. F. 1963, *Observatory*, **83**, 255.
———. 1968, *A Photometric Atlas of the Spectrum of Arcturus* (Cambridge, England: Cambridge Philosophical Society).
Griffin, R., and Griffin, R. 1967, *M.N.R.A.S.*, **137**, 253.
Gustafsson, B., Kjaergaard, P., and Anderson, S. 1974, *Astr. and Ap.*, **34**, 99.
Hayes, D. S. 1967, unpublished Ph.D. thesis, University of California, p. 57.
Hoffleit, D. 1964, *Catalogue of Bright Stars* (New Haven: Yale University Obs.).
Hummer, D. G. 1968, *M.N.R.A.S.*, **141**, 479.
Iben, I., Jr. 1967, *Ann. Rev. Astr. and Ap.*, **5**, 571.
Johnson, H. R. 1973, unpublished.
Kondo, Y., Giuli, R. T., Modisette, J. L., and Rydgren, A. E. 1972, *Ap. J.*, **176**, 153.
Kraft, R. P. 1959, *Ann. d'Ap.*, **22**, 164.
Kunasz, P. B. 1973, unpublished Ph.D. thesis, University of Colorado.
Kuperus, M. 1965, *Res. Astr. Obs. Utrecht*, **17**, 1.
Latham, D. W. 1970, *Smithsonian Ap. Obs. Spec. Rept.*, No. 321 (Ph.D. thesis, Harvard University).
Liller, W. 1968, *Ap. J.*, **151**, 589.
Linsky, J. L., and Avrett, E. H. 1970, *Pub. A.S.P.*, **82**, 169.
Linsky, J. L., and Ayres, T. R. 1973, *Ap. J.*, **180**, 473 (Paper I).
Linsky, J. L., Basri, G., McClintock, W., Henry, R. C., and Moos, H. W. 1974, *Bull. AAS*, **6**, 458.
Linsky, J. L., McClintock, W., Henry, R. C., Moos, H. W., Gerola, H., and Shine, R. A. 1975, submitted to *Ap. J.*
Lutz, T. E., Furenlid, I., and Lutz, J. H. 1973, *Ap. J.*, **184**, 787.
Mihalas, D. 1970, *Stellar Atmospheres* (San Francisco: Freeman).
Milkey, R. W., Ayres, T. R., and Shine, R. A. 1975*a*, *Ap. J.*, **197**, 143.
Milkey, R. W., and Mihalas, D. 1973*a*, *Ap. J.*, **185**, 709.
———. 1973*b*, *Solar Phys.*, **32**, 361.
———. 1974, *Ap. J.*, **192**, 769.
Milkey, R. W., Shine, R. A., and Mihalas, D. 1975*b*, *Ap. J.* (in press).
Modisette, J. L., Nichols, R. E., and Kondo, Y. 1973, *Ap. J.*, **186**, 219.
Moos, H. W., Linsky, J. L., Henry, R. C., and McClintock, W. 1974, *Ap. J.* (*Letters*), **188**, L93.
Moos, H. W., and Rottman, G. J. 1972, *Ap. J.* (*Letters*), **174**, L73.
Mount, G. H., Ayres, T. R., and Linsky, J. L. 1975, *Ap. J.* (in press).
Mount, G. H., and Linsky, J. L. 1974, *Solar Phys.*, **35**, 259.
Noyes, R. W., and Kalkofen, W. 1970, *Solar Phys.*, **15**, 120.
Oke, J. B. 1964, *Ap. J.*, **140**, 689.
Pasachoff, J. M., and Lepler, F. C. 1972, *Bull. AAS*, **4**, 235.
Reimers, D. 1973, *Astr. and Ap.*, **24**, 79.
Roman, N. G. 1952, *Ap. J.*, **116**, 122.
———. 1955, *Ap. J. Suppl.*, **2**, 198.
Scharmer, G. B. 1974, submitted for publication.
Shine, R. A. 1973, unpublished Ph.D. thesis, University of Colorado.
Shine, R. A., and Linsky, J. L. 1974*a*, *Solar Phys.*, **37**, 145.
———. 1974*b*, *Solar Phys.* (in press).
Shine, R. A., Milkey, R. W., and Mihalas, D. 1975, *Ap. J.* (in press).
Shine, R. A., and Oster, L. 1973, *Bull. AAS*, **5**, 279.
Simon, T. 1970, unpublished Ph.D. thesis, Harvard University.
Simon, T., Morrison, D., and Cruikshank, D. P. 1972, *Ap. J.* (*Letters*), **177**, L17.
Smith, M. A. 1974, *Ap. J.*, **192**, 623.
Thomas, R. N., and Athay, R. G. 1961, *Physics of the Solar Chromosphere* (New York: Interscience).
Ulmschneider, P. 1967, *Zs. f. Ap.*, **67**, 193.
van Paradijs, J., and Meurs, E. J. A. 1974, *Astr. and Ap.*, **35**, 225.
Vaughan, A. H. Jr., and Zirin, H. 1968, *Ap. J.*, **152**, 123.
Vernazza, J. E., Avrett, E. H., and Loeser, R. 1973, *Ap. J.*, **184**, 605.
White, O. R., and Suemoto, Z. 1968, *Solar Phys.*, **3**, 523.
Willstrop, R. V. 1965, *Mem. R.A.S.*, **69**, 83.
———. 1972, private communication.
Wilson, O. C. 1938, *Pub. A.S.P.*, **50**, 245.
———. 1957, *Ap. J.*, **126**, 46.
———. 1966, *Science*, **151**, 1487.
———. 1972, concluding remarks, Stellar Chromosphere Conference, NASA SP-371, p. 311.
Wilson, O. C., and Bappu, M. K. V. 1957, *Ap. J.*, **125**, 661.

*Note added in proof.*—Recently, Mäckle, Holweger, Griffin, and Griffin (*Astr. and Ap.*, **38**, 239 [1975]) have proposed a model photosphere for Arcturus based on the measured shapes of strong line wings and equivalent widths. Assuming LTE, they derive a much lower surface gravity $\log g = 0.90 \pm 0.35$ than the value of $\log g = 1.7$ proposed in previous work and adopted here. Since their value of the gravity implies a very low mass for Arcturus—in apparent conflict with stellar evolution theory—and since their model is based on the same type of data as ours, we feel obliged to make the following comments concerning it.

1. The effect of partial coherent scattering is to lower the source function in the damping wings of strong resonance lines (cf. Fig. 7). Thus one can accurately match the same wing data with LTE–CRD photospheric models cooler at equivalent mass column densities than the corresponding PRD model (cf. Fig. 9), and indeed the Mäckle *et al.* ($T_{\rm eff} = 4260$ K, $\log g = 0.9$) model is systematically cooler than ours by 90–170 degrees for $2 \leq m \leq 40$ where the Ca II wings are formed.

2. The Mäckle *et al.* gravity is derived by requiring that the equivalent widths of neutral and ionized atoms yields the same abundances; in other words, by ionization balance considerations. If the photospheric "basis" temperatures are systematically low and if no allowance for a chromospheric temperature rise is made, then ionization

balance cannot yield the same abundances for neutral and ionized species unless the pressure for a given temperature is decreased. This is possible only for values of the gravity which are also too low. In fact, by this method the derived gravity is a sensitive function of the effective temperature *scaling factor* for the adopted photospheric temperature distribution, and decreases an order of magnitude for only a 200 K decrease in $T_{\rm eff}$. Thus, an underestimate of the upper photosphere temperature distribution by only 4 percent will account for an underestimate of 0.8 in log $g$.

3. However, our method of deriving photospheric temperature distributions from a PRD analysis of Ca II line wings is itself relatively insensitive to the assumed value of the gravity and cannot be used to derive log $g$. We have synthesized PRD damping wing profiles of K for the tabulated Mäckle *et al.* model and find reasonable agreement with the empirically calibrated profile to within the $\pm 30$ percent accuracy cited in § II. Therefore, we cannot rule out the low gravity they derive on this basis alone.

4. If log $g = 0.9$ instead of 1.7, then the major effect on our calculations would be to lower the estimated strengths of the ultraviolet transition region and coronal emission lines since our inferred values of $m_0$ are relatively insensitive to the gravity.

T. R. Ayres: Center for Astrophysics, 60 Garden St., Cambridge, MA 02138

J. L. Linsky: Joint Institute for Laboratory Astrophysics, University of Colorado, Boulder, CO 80302